the size decreases even in the case of desolvation. To be able to predict more precisely when and how much Knudsen effect contributes to desolvation, the entire life of mono-dispersed droplets should be monitored and this study is underway in our laboratory.

Acknowledgment. The authors are grateful for the financial support by the Korean Science and Engineering Foundation (94-0800-03-02).

References

1. Boorn, A. W.; Cresser, M. S.; Browner, R. F. *Spectrochim. Acta,* **1980**, *35B*, 823.
2. Clampitt, N. C.; Hieftje, G. M. *Anal. Chem.* **1972**, *44*, 1211.
3. Bastiaans, G. J.; Hieftje, G. M. *Anal. Chem.* **1974**, *46*, 901.
4. Hieftje, G. M.; Wittig, E.; Pak, Y.; Miller, J. M. *Anal. Chem.* **1987**, *59*, 2867.
5. Chen, X.; Pfender, E. *Plasma Chem. Plasma Process.* **1982**, *2*, 293.
6. Chen, X.; Pfender, E. *Plasma Chem. Plasma Process.* **1983**, *3*, 97.
7. Chen, X.; Pfender, E. *Plasma Chem. Plasma Process.* **1982**, *3*, 351.
8. Russo, R. E.; Hieftje, G. M. *Anal. Chim. Acta,* **1980**, *118*, 293.
9. Hottel, H. C.; Williams, G. C.; Simpson, H. C. *Fifth Symposium on Combustion*; Reinhold: New York, 1955; 101.
10. Bahn, G. S. *Advances in Chemistry Series,* **1958**, *2*, 104.
11. Monchick, L.; Reiss, H. *J. Chem. Phys.* **1954**, *22*, 831.
12. Hirshfelder, J. O.; Curtiss, C. O.; Bird, R. B. *Molecular Theory of Gases and Liquids*; Wiley & Sons: New York, N. Y., 1954; p 526.
13. *JANAF*, 2nd ed.; U. S. Government Printing Office: Washington, D. C., 1971.
14. *International Critical Tables*, 1st ed.; McGraw-Hill: New York and London, 1926.
15. Hirth, J. P. *In the Characterization of High Temperature Vapors*; Margrave, J. L., Ed.; Wiley: New York, 1967; p 453.

Determination of Electron Transfer Kinetics at Ferrocenecarboxamidoyl Monolayer/Solution Interface

Hun-Gi Hong

Department of Chemistry,
Sejong University,
Seoul 133-747, Korea

Received June 17, 1996

Monomolecular film of self-assemblies[1~7] has been used as a model system to understand complex interfacial phenomena such as wetting, adhesion, friction, catalysis and electron/energy transfer on biological membrane. The electron transfer kinetics at the redox-polymer/ solution interface have been already extensively studied in both theoretical and experimental approaches by Saveant, Anson, Murray, Albery and their coworkers.[8~12] However, there are only a few reports[1a,13,14] on the electron transfer in self-assembled electroactive monolayers. Recently, we reported electrochemical measurements of electron transfer rates on the redox-active molecule-terminated film based on zirconium phosphonate.[15] This note reports indirect determination of kinetic parameters for the mediated electron transfer reaction between ferrocenecarboxamidoyl monolayer film and solution species. In order to get the kinetic information on monolayer-coated electrode system, it is essential to take into account simultaneously a few factors which can limit current. The rate constant for electron-cross exchange (k_{ex}), standard rate constant ($k°$) and symmetry factor (α) which were related to several limiting factors such as mass transfer, electron-exchange and charge transport were determined from observed limiting currents (i_{obs}) by digital simulation using three parameters-fit least squares.

Results and Discussion

The sequential adsorption procedure[6,15] was used to prepare gold rotating disk electrode modified with electroactive ferrocenecarboxamidoyl monolayer. This modified Au electrode typically gives well-defined surface waves (shown in Figure 1) in which peak current is linearly proportional to scan rate (data not shown) and peak potential separation was smaller than 30 mV independent of scan rate between 20 and 200 mV/s. The surface formal potential (E''_s) of ferro-

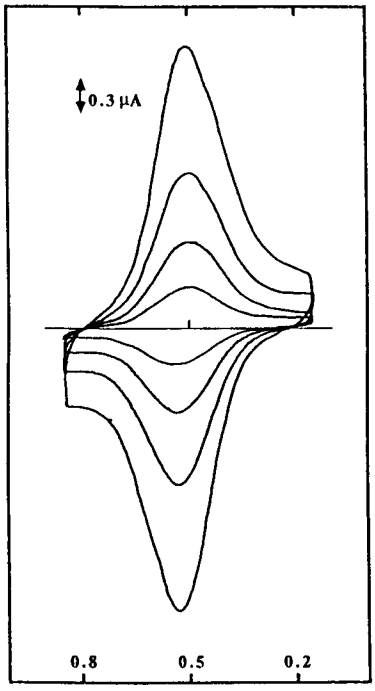

Figure 1. Cyclic voltammograms of ferrocene-modified Au electrode in 0.1 M $NaClO_4$. Potential, V *vs.* SCE.

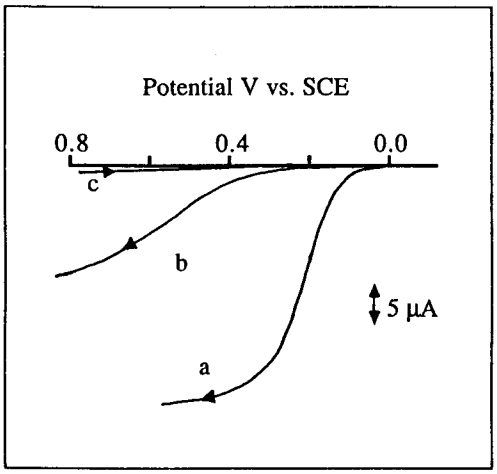

Figure 2. (a) Current-potential curve at a bare Au rotating disk electrode in 1 mM $Fe(CN)_6^{4-}$, 0.1 M $NaClO_4$. Current-potential curves of ferrocene-modified Au rotating disk electrode in 0.1 M $NaClO_4$: (b) in 1.0 mM $Fe(CN)_6^{4-}$; (c) in 1.0 mM $Fe(CN)_6^{3-}$. All scan rates and rotation rates were 2 mV /s and 1600 rpm.

cene is 0.50± 0.02 V *vs.* SCE. The charge passed in the anodic and cathodic waves indicates surface coverages of redox molecule in the range of $(2\text{-}6)\times 10^{-10}$ mol/cm^2. These voltammetric behaviors were investigated more clearly by using Au rotating disk electrode (RDE) in 0.1 M $NaClO_4$ aqueous solution containing ferro/ferricyanide as redox couple. Ferro/ferricyanide was selected as an electrochemical probe because it is an electrochemically reversible, one-electron outer-sphere redox couple.

Figure 2 shows hydrodynamic current-potential curves obtained at bare gold and ferrocene-terminated Au RDE. As expected, the limiting current due to oxidation of $Fe(CN)_6^{4-}$ is observed at bare Au RDE (shown in Figure 2a) and its half wave potential ($E_{1/2}$) is almost same as reported $E^{0\prime}$ (0.20 V) of $Fe(CN)_6^{4-}$. However, in Figure 2b, the oxidation of $Fe(CN)_6^{4-}$ barely starts around 0.24 V on the Au rotating disk electrode modified with ferrocene. This electrode shows kinetically limited quasi-reversible voltammogram, which demonstrates clearly that the ferricenium cation, electrochemically generated on Au electrode, oxidizes $Fe(CN)_6^{4-}$ in solution phase by mediation (eq. 1).

$$\text{Ferricenium}^{+} + Fe(CN)_6^{4-} = \text{Ferrocene} + Fe(CN)_6^{3-} \quad (1)$$

The large $E_{1/2}$ shift in *i-E* waves(Figure 2a and 2b) results from the existence of zirconium phosphonate film because the film blocks direct electron transfer between the electrode and solution redox couple. Therefore, the presence of electroactive film enhances the bloking capabilities of the layer for direct $Fe(CN)_6^{4-}$ oxidation, while simultaneously promoting the mediated oxidation of $Fe(CN)_6^{4-}$ through the ferrocene-ferricenium redox state. Figure 2c was recorded in 1 mM solution of $Fe(CN)_6^{3-}$ on ferrocene-modified Au RDE. No faradaic current was observed except background charging current in the negative scan direction. This indicates that the reduction of ferricyanide by the immobilized ferrocene is thermodynamically unfavorable.

Figure 3 shows basic electron-relay regarding mediated electron-cross exchange reaction at redox-monomer/ solution

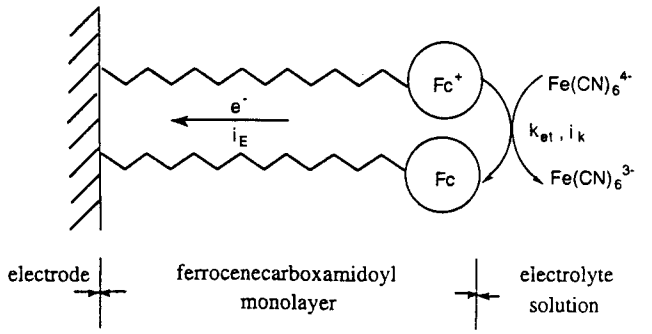

Figure 3. Mediated electron cross-exchange redox reaction of a solution redox species at ferrocenecarboxamidoyl monolayer-modified Au rotating disk electrode.

interface. The electrons are relayed to the electrode surface through the film. For this system, the overall electron transfer consists of electron cross-exchange reaction kinetics, charge transport at the film/electrode interface, and mass transfer of solution redox molecule. Therefore, all of three processes should be taken into consideration as current limiting factors to yield kinetic informations. This problem exactly belongs to "the case C" which has been theoretically elucidated in detail by Anson and Saveant and their coworkers.[8] The experimentally observed limiting current (i_{obs}) should be analyzed by the interplay of the current-limiting factors in order to get the rate constant (k_{et}) for the electron-cross exchange reaction, symmetry factor (α) and standard rate constant (k^0) for the irreversible film/electrode reaction.

The i_{obs} at a Au RDE modified with ferrocene molecular array is related to i_K, i_L by Eq. (2)[8,12]

$$1/i_{obs} = 1/i_L + 1/i_E + 1/i_K + (1/K_{eq} - 1)\ i_{obs}/i_E\ i_L \quad (2)$$

where i_L is the Levich or solution mass transport limited current, i_E is the film/electrode reaction current, i_K is the film/solution electron cross exchange reaction current and K_{eq} is the equilibrium constant for the cross-exchange redox reaction occuring at film/solution interface. The mediated oxidation of $Fe(CN)_6^{4-}$ is thermodynamically favored by approximately 300 mV so that the reverse reaction may be considered to have a negligible effect. As a result, the equilibrium constant ($K_{eq} \gg 1$) is very large and allows Eq. (2) to be simplified Eq. (3),

$$1/i_{obs} = 1/i_L + 1/i_E + 1/i_K - i_{obs}/i_E\ i_L \quad (3)$$

Here i_L is given by the Levich Eq. (4)

$$i_L = 0.617\ nFAD^{2/3}\omega^{1/2}\nu^{-1/6}C^* \quad (4)$$

where A is electrode area, D is diffusion coefficient, ω is rotation rate, ν is kinematic viscosity and C^* is bulk concentration of solution species. For the irreversible film/electrode reaction,

$$i_E = nFAk_fC^* \quad (5)$$

where $k_f = k^0 \exp[(1-\alpha)\eta nF/RT]$ and i_E is dependent of overpotential ($\eta = E\text{-}E^{0\prime}$). The relation between the kinetics limited current i_K and the rate constant k_{et} is given by Eq. (6)

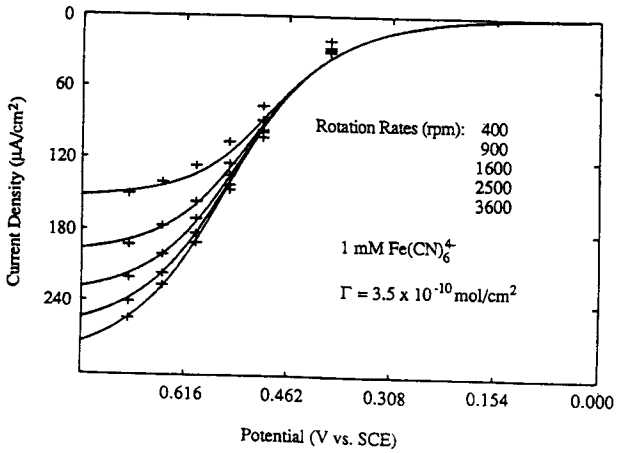

Figure 4. The simulated current-potential curves (represented in solid lines) which gave the best fit to experimentally observed limiting currents (marked in cross points). Surface coverage (Γ) value of ferrocene moiety of modified electrode used in voltammetric experiment was 3.5×10^{-10} mol/cm^2.

$$i_K = nFAk_{et}C^*\Gamma^* \quad (6)$$

where Γ^* is the surface coverage of ferrocene and k_{et} is expressed as a bimolecular rate constant. Plugging known values of $D(=7\times10^{-6}$ cm^2/s), $C^*(=1.0$ mM), $A(=0.07$ cm^2), $\Gamma(=3.5\times10^{-10}$ mol/cm^2), and $\nu(=0.01$ cm^2/s) into the last 4 equations leaves only three unknown values (k_{et}, k^o, and α). Figure 4 shows the best current -potential simulation curves obtained from least squares fit to experimental data at rotation rates from 400 to 3600 rpm. The simulation curves fit the experimental current-potential points (represented by "+" in Figure 5) quite well in the high overpotential region. This simple simulation yields useful kinetic informations such as $k_{et}=1.5(\pm0.2)\times10^7$ cm^3 mol^{-1} s^{-1}, $k^o=3.5(\pm0.3)$ s^{-1} and $\alpha=0.32(\pm0.07)$. In the low overpotential region (<0.4 V *vs.* SCE), the simulation curves show that a small current independent of rotation speed and overpotential flows. This deviation seems to be due to a small amount of permeation of solution redox molecule through structural defect sites in electroactive monolayer. Another reason might be ascribed to small value of K_{eq} so that $1/K_{eq}$ term in Eq. (2) is no longer approximately to zero. The value of k_{et} obtained in this study is in quantitative agreement with theory[8] in that the practical upper limit[9] for reliable measurements of k_{et} at RDE is about 5×10^8 cm^3 mol^{-1} s^{-1}. The value of standard rate constant, k^o, for the irreversible charge transfer reaction at film/electrode interface is independent of overpotential and is dependent of film thickness. The distance from the electrode surface to ferrocene layer was estimated to be 28.7 (± 2.4) Å by ellipsometry. The values of k^o and film thickness obtained in this study is quite close to those reported by Chidsey *et al.*[13] They found the value of $k^o=1.8$ s^{-1}, which was measured from monolayer of alkanethiol terminated with ferrocene in which film thickness is *ca.* 30 Å. This fact seems to insinuate that electron tunneling through dielectric film would be involved in the transport of charge resulting from mediated-oxidation of solution redox molecule.

Experimental

Reagents and materials. Ferrocenecarboxylic acid, zirconyl chloride octahydrate, 1,4-dibromobutane, triethyl phosphite, diethyl phosphite, 4-iodoaniline, bromotrimethylsilane and oxalyl chloride were used as received from Aldrich Chemical Co. $K_4Fe(CN)_6$ and $K_3Fe(CN)_6$ (Mallinckrodt), $NaClO_4$ (Fisher) were used as received. CH_3CN and CH_2Cl_2 were refluxed over P_2O_5 and distilled before use. The preparation of ferrocenecarboxamidoyl[$=Fe(C_6H_5)(C_6H_4$-CO-NH-)] monolayer on Au RDE was achieved by the sequential adsorption of MBPA, Zr(IV), and [4-(ferrocenecarboxamido)phenyl]-phosphonic acid(FcPP)[16] as previously reported.[6,15] Rotating disk electrode was home-fabricated from a 0.025 mm-thick Au foil and teflon tubings (0.5″ and 0.25″ in outer diameter).

Instrumentation. Electrochemical measurements were carried out with rotating gold disk electrode, platinum flag counter electrode and a SCE in one-compartment specially designed cell which can remove the air bubbles formed during the rotation. EG&G/PAR 273A potentiostat, RE 0151 x-y recorder and Pine Instrument Rotator were used to record voltammograms. Ellipsometric measurements were made using a Gaertner model L2W26D ellipsometer with 6328 Å (He-Ne laser) analyzing light and a rotating analyzer. A simple Basic program for simulation was written to extract kinetic parameter values from experimentally observed limiting currents.

Acknowledgment. This work was supported by NON DIRECTED RESEARCH FUND, Korea Research Foundation, 1994. And also the present study was supported in part by the Basic Science Research Institute program, Ministry of Education, Korea, 1994, Project No. 94-3430.

References

1. (a) Porter, M. D.; Bright, T. B.; Allara, D. L.; Chidsey, C. E. D. *J. Am. Chem. Soc.* **1987**, *109*, 3559. (b) Nuzzo, R. G.; Allara, D. L. *J. Am. Chem. Soc.* **1983**, *105*, 4481.
2. (a) Finklea, H. O.; Avery, S.; Lynch, M.; Furtsch, T. *Langmuir* **1987**, *3*, 409. (b) Finklea, H. O.; Robinson, L. R.; Blackburn, A.; Richter, B.; Allara, D.; Bright, T. B. *Langmuir* **1986**, *2*, 239.
3. Allara, D. L.; Nuzzo, R. G. *Langmuir* **1985**, *1*, 52.
4. Tillman, N.; Ulman, A.; Penner, T. L. *Langmuir* **1989**, *5*, 101.
5. Maoz, R.; Sagiv, J. *J. of Colloid and Interface Sci.* **1984**, *100*, 465.
6. Lee, H.; Kepley, L. R.; Hong, H.-G.; Akhter, S.; Mallouk, T. E. *J. Phy. Chem.* **1988**, *92*, 2597.
7. (a) Dines, M. B.; DiGiacomo, P. *Inorg. Chem.* **1981**, *20*, 92. (b) Dines, M. B.; Cooksey, R. E.; Griffith, P. C. *Inorg. Chem.* **1983**, *22*, 1003.
8. (a) Andrieux, C. P.; Dumas-Bouchiat, J. M.; Saveant, J. M. *J. Electroanal. Chem.* **1982**, *131*, 1. (b) Andrieux, C. P.; Saveant, J. M. *J. Electroanal. Chem.* **1982**, *134*, 163. (c) Andrieux, C. P.; Saveant, J. M. *J. Electroanal. Chem.* **1982**, *142*, 1. (d) Anson, F. C.; Saveant, J. M.; Shigehara, K. *J. Phy. Chem.* **1983**, *87*, 214.
9. (a) Denisevich, P.; Willman, K.; Murray, R. W. *J. Am. Chem. Soc.* **1981**, *103*, 4727. (b) Ikeda, T.; Leidner, C. R.; Murray, R. W. *J. Am. Chem. Soc.* **1981**, *103*, 7422. (c) Ikeda, T.; Schmehl, R.; Denisevich, P.; Willman, K.; Murray, R. W. *J. Am. Chem. Soc.* **1982**, *104*, 2683. (d)

Rocklin, R. D.; Murray, R. W.; Andrieux, C. P.; Saveant, J. M. *J. Electroanal. Chem.* **1982**, *134*, 163.
10. Albery, W. J.; Hillman, A. R. *J. Electroanal. Chem.* **1984**, *170*, 27.
11. (a) Oyama, N.; Anson, F. C. *J. Am Chem. Soc.* **1979**, *101*, 739. (b) Oyama, N.; Anson, F. C. *Anal. Chem.* **1980**, *52*, 1192.
12. Mallouk, T. E.; Cammarata, V.; Crayston, J. A.; Wrighton, M. S. *J. Phy. Chem.* **1986**, *90*, 2150.
13. (a) Chidsey, C. E. D.; Bertozzi, C. R.; Putvinski, T. M.; Mujsce, A. M. *J. Am. Chem. Soc.* **1990**, *112*, 4301. (b) Chidsey, C. E. D. *Science* **1991**, *251*, 919.
14. Finklea, H. O.; Hanshew, D. D. *J. Am. Chem. Soc.* **1992**, *114*, 3173.
15. (a) Hong, H.-G.; Mallouk, T. E. *Langmuir* **1991**, *7*, 2362. (b) Hong, H.-G. *Bull. Korean Chem. Soc.* **1995**, *16*, 886.
16. FcPP was prepared from diethyl (*p*-aminophenyl)phosphonate (2.2 g, 10 mmole), ferrocenoyl chloride (2.5 g, 10 mmole) and dry triethylamine (1.5 mL, 10 mmole) dissolved in 20 mL of dry THF. The fine yellow powder (4.2 g, 98% yield) was identified as diethyl [4-(ferrocenecarboxamido)phenyl]phosphonate by ^{1}H NMR. After the diethyl group of this compound was replaced by bis(trimethylsilyl), the silyl ester (0.53 g, 1 mmole) was redissolved and refluxed in 70 mL of methanol. Finally the potassium salt of [4-(ferrocenecarboxamido)phenyl]phosphonic acid was precipitated by addition of methanolic KOH solution. The precipitate was washed by neat methanol, dried under vacuum and identified by proton nmr.

Effect of Hydrochloric Acid Concentrations on the Hydride Generation Efficiencies in ICP-AES

Dong Kee Lee* and Beom Suk Choi†

**Korea Testing and Research Institute for Chemical Industry, Seoul 150-038, Korea*
†Department of Chemisty and Institute of Basic Sciences, Kyung Hee University, Yongin 449-701, Korea

Received June 24, 1996

The hydride generation (HG) technique has been used extensively as a means of efficient sample introduction to improve detection limit for hydride forming elements in inductively coupled plasma (ICP)-atomic emission spectrometry (AES). The method was first described by Thompson *et al.*,[1~4] who established the best compromise conditions for the generation of hydrides from hydrochloric acid and sodium borohydride solutions. On the other hand, sodium hydroxide is always used to prevent decomposition of sodium borohydride solution.[5]

The solution of pH has a significant effect on the hydride generation process, and the optimum pH regions for all hydride forming elements have been reported.[1~4] However, those are almost exclusively experimental studies. A theoretical prediction of the effect of pH on hydride generation has not yet been studied.[6~7] In the present study, we used a continuous HG-ICP-AES system and studied the molarity relationship between reactants: acid, sodium borohydride and sodium hydroxide.

Experimental

Instrument. All measurements were carried out with a Labtam model 8440 ICP spectrometer in conjuction with a Labtam model 8440 continuous hydride generator.[8] The experimental conditions used are summarized in Table 1. The peristaltic pumps used are the Minipuls 2 (Gilson) for the acidic sample solution and KSC 1303-P2 (Manhattan) for the basic reductant solution. The experimental errors for the measurement of the flow rates ranged 5-8%.

Reagent. All reagents were of analytical grade or higher purity, and the deionized water from Milli Q system (Millipore) was used. 1000 ppm of standard stock solutions of As(V), Bi(V), Ge(IV), Sb(V), Sn(IV) were obtained from Junsei Chemical Co. Ltd., and the diluted solution were prepared with a fixed acid solutions (0.05~4.0 M) immediately before use. Sodium borohydride solution was prepared by dissolving the powder (Aldrich) in deionized water containing 0.1% or 2.5% NaOH. The solution was filtered to eliminate turbidity and it was stable for 1 day.

Results and Discussion

In order to investigate the relationship between the concentrations of reactants, a series of analyte solutions containing different concentrations of HCl (0.05~4.0 M) were prepared. The solutions were reacted with the three cases of reduction

Table 1. Specifications and operation conditions of ICP

RF generator	27.12 MHz
RF power	1.4 kW
Observation height	6 mm above RF coil
Spectrometer	Czerny Turner type, Vacuum
	1800 grooves/mm
	0.01 nm/mm (2nd order)
Slit width	0.02 mm
PMT voltage	1.0 kV
Gas flow rate	Carrier 0.8 L/min
	Coolant 13 L/min
	Auxiliary 0.4 L/min
Wavelength (nm)	As 193.696
	Bi 223.061
	Ge 209.425
	Sb 217.581
	Sn 189.989